Profiling and relative quantification of multiply nitrated and oxidized fatty acids

Ivana Milic, Eva Griesser, Venukumar Vemula, Naoya Ieda, Hidehiko Nakagawa, Naoki Miyata, Jean-Marie Galano, Camille Oger, Thierry Durand, Maria Fedorova

Profiling and relative quantification of multiply nitrated and oxidized fatty acids

Ivana Milic[1,2] · Eva Griesser[1,2] · Venukumar Vemula[1,2] · Naoya Ieda[3] · Hidehiko Nakagawa[3,4] · Naoki Miyata[3] · Jean-Marie Galano[5] · Camille Oger[5] · Thierry Durand[5] · Maria Fedorova[1,2]

Received: 13 March 2015 / Revised: 30 April 2015 / Accepted: 5 May 2015

Abstract The levels of nitro fatty acids (NO_2-FA), such as nitroarachidonic, nitrolinoleic, nitrooleic, and dinitrooleic acids, are elevated under various inflammatory conditions, and this results in different anti-inflammatory effects. However, other multiply nitrated and nitro-oxidized FAs have not been studied so far. Owing to the low concentrations in vivo, NO_2-FA analytics usually relies on targeted gas chromatography–tandem mass spectrometry (MS/MS) or liquid chromatography–MS/MS, and thus require standard compounds for method development. To overcome this limitation and increase the number and diversity of analytes, we performed in-depth mass spectrometry (MS) profiling of nitration products formed in vitro by incubating fatty acids with NO_2BF_4, and $ONOO^-$. The modified fatty acids were used to develop a highly specific and sensitive multiple reaction monitoring LC–MS method for relative quantification of 42 different nitrated and oxidized species representing three different groups: singly nitrated, multiply nitrated, and nitro-oxidized fatty acids. The method was validated in in vitro nitration kinetic studies and in a cellular model of nitrosative stress. NO_2-FA were quantified in lipid extracts from 3-morpholinosydnonimine-treated rat primary cardiomyocytes after 15, 30, and 70 min from stress onset. The relatively high levels of dinitrooleic, nitroarachidonic, hydroxynitrodocosapenataenoic, nitrodocosahexaenoic, hydroxynitrodocosahexaenoic, and dinitrodocosahexaenoic acids confirm the presence of multiply nitrated and nitro-oxidized fatty acids in biological systems for the first time. Thus, in vitro nitration was successfully used to establish a targeted LC–MS/MS method that was applied to complex biological samples for quantifying diverse NO_2-FA.

Keywords Cardiomyocytes · Lipid nitration · Lipid peroxidation · Nitrated fatty acids · Nitrosative stress

Electronic supplementary material The online version of this article (doi:10.1007/s00216-015-8766-3) contains supplementary material, which is available to authorized users.

✉ Maria Fedorova
maria.fedorova@bbz.uni-leipzig.de

[1] Faculty of Chemistry and Mineralogy, Institute of Bioanalytical Chemistry, Leipzig, Germany

[2] Center for Biotechnology and Biomedicine, Universität Leipzig, Deutscher Platz 5, 04103 Leipzig, Germany

[3] Graduate School of Pharmaceutical Science, Nagoya City University, 3-1, Tanabe-dori, Mizuho-ku, Nagoya, Aichi 467-8603, Japan

[4] PRESTO, Japan Science and Technology Agency, 4-1-8 Honcho, Kawaguchi, Saitama 332-0012, Japan

[5] Institut des Biomolécules Max Mousseron, Université de Montpellier, ENSCM, CNRS UMR 5247, Montpellier, France

Introduction

Nitric oxide (•NO) is a well-known mediator of various biological processes [1]. Besides being a potent vasodilator, •NO is generated by phagocytes as part of the innate immune response [2] preventing platelet aggregation [3, 4] and leukocyte adhesion to the endothelium [5]. Under aerobic conditions, nitric oxide readily reacts with reactive oxygen species (ROS) yielding various reactive nitrogen species (RNS) [6]. Whereas some RNS can act as oxidants and nitrosylating agents (NO^+, N_2O_3, etc.), nitrogen dioxide radical ($•NO_2$), peroxynitrite anion ($ONOO^-$), and nitronium cation (NO_2^+) are known nitrating species. The concentrations of •NO and

oxygen in the hydrophobic environment of cellular membranes and the lipid core of lipoproteins can be several times higher than in the cytoplasm, triggering elevated RNS production rates. In fact, around 90 % of •NO is auto-oxidized in these compartments [7, 8] and this can modify surrounding biomolecules. Free polyunsaturated fatty acids (PUFA) and their esters are the primary targets of RNS owing to their high susceptibility to oxidation and nitration.

In vivo formation of nitrated fatty acids (NO_2-FA) was supported by their detection in human blood plasma [9–13], membranes of red blood cells [14], and urine [15, 16]. Recent evidence indicates increased nitroalkene production rates in various inflammatory models, such as a 20-fold higher cholesteryl nitrolinoleate level in murine J774.1 macrophages activated by an inflammatory stimulus [17]. Increased levels of nitrolinoleic acid ($LaNO_2$) were detected in mitochondria during ischemic preconditioning, whereas the level of nitrooleic acid ($OaNO_2$) remained unchanged, indicating possible selectivity of fatty acid nitration [18]. Under inflammatory conditions $LaNO_2$, $OaNO_2$, and nitroarachidonic acid ($AaNO_2$) posses anti-inflammatory activities [19–21], including activation of peroxisome-proliferator-activated receptors [22] and nuclear factor E2 related factor 2 [23, 24], induction of heme oxygenase 1 [25], inhibition of nuclear factor κB, and inhibition of prostaglandin endoperoxide H synthase (PGHS) [26] and NADPH oxidase [27]. $OaNO_2$ decreased superoxide production in activated macrophages and pulmonary artery smooth muscle cells, demonstrating protective effects in a hypoxia-induced murine model of pulmonary hypertension [28]. Additionally, $OaNO_2$ reduced atherosclerotic lesion formation in apolipoprotein E deficient mice by inhibiting vascular smooth muscle cell proliferation [29]. Recently it was demonstrated that $OaNO_2$ effectively induces expression of heat shock proteins and antioxidant enzymes in keratinocytes [30]. Synthetic $AaNO_2$ revealed several new regulatory properties in cellular models that might be common for NO_2-FA. Release of nitric oxide by $AaNO_2$ can induce cyclic GMP (cGMP)-dependent vasorelaxation and downregulate inducible nitric oxide synthase [31]. Additionally, $AaNO_2$ was shown to prevent NADPH oxidase assembly [27], regulate protein kinase C [32], and inhibit oxygenase activities of PGHS-1 and PGHS-2.

Despite increasing interest in the therapeutic potential of NO_2-FA, their in vivo diversity has not been fully discovered. Currently, data are limited to $LaNO_2$, $OaNO_2$, and $AaNO_2$, whereas other possible modifications—for example, polynitro-PUFA and hydroxynitro-PUFA—have rarely been addressed. In vivo, ROS and RNS are produced simultaneously, and it is likely that oxidation of PUFA can be followed by their nitration, and vice versa, leading to a higher diversity of modified PUFA than is currently assumed. Owing to their very low in vivo concentrations, ranging from high picomolar to low nanomolar concentrations, mass-spectrometric detection of NO_2-FA is very challenging. Therefore, multiple reaction monitoring (MRM) is often used to achieve the required sensitivity. However, MRM allows only targeted detection, and is thus limited to known or expected compounds. It does not provide information on NO_2-FA diversity. To overcome these limitations, we performed an in-depth profiling of PUFA [oleic acid (Oa), linoleic acid (La), conjugated La (cLa), arachidonic acid (Aa), and docosahexaenoic acid (Dha)] nitrated in vitro under low and high oxygen tension to monitor the kinetics of NO_2-FA. On the basis of the diversity of NO_2-FA identified in vitro, a highly specific and sensitive liquid chromatography (LC)–tandem mass spectrometry (MS/MS) MRM method was developed and applied for the detection and relative quantification of NO_2-FA in a cardiomyocyte cell model of nitrosative stress.

Materials and methods

Chemicals

All unsaturated fatty acids, *tert*-butyl methyl ether (MTBE), lithium trifluoroacetate, and horse serum were purchased from Sigma-Aldrich (Taufkirchen, Germany). Acetonitrile, methanol, and ammonium formate [ultrapure LC/mass spectrometry (MS) grade] were obtained from Biosolve (Valkenswaard, Netherlands). Chloroform was purchased from Merck (Darmstadt, Germany). 2,3,5,6-Tetramethyl-4-(methylnitrosoamino)phenol (P-NAP) was synthesized according to Ieda et al. [33]. C_{21}-15-F_{2t}-IsoP, d_4-10-F_{4t}-NeuroP, and d_4-4-RS-4-F_{4t}-NeuroP were synthesized according to the published procedure [34, 35]. Dulbecco's modified Eagle's medium/Ham's F12 medium was purchased from PAA Laboratories (Cölbe, Germany). Fetal bovine serum, phosphate-buffered saline, L-glutamine, nonessential amino acids, sodium pyruvate, and antibiotic (penicillin/streptomycin) solutions were obtained from Life Technologies (Darmstadt, Germany). 3-Morpholinosydnonimine (SIN-1) was purchased from Enzo Life Sciences (Lörrach, Germany).

PUFA nitration by NO_2BF_4

Oa, La, Aa, and Dha (100 g/L in chloroform) were nitrated in the presence of solid nitronium tetrafluoroborate (NO_2BF_4; 100 mg, PUFA–NO_2BF_4, 1:2 molar ratio, 20 °C, 1 h, intense shaking). Nitration was quenched (0.5 mL of deionized water; vortexing for 30 s), and the lower organic phase was dried under a vacuum and reconstituted in chloroform (1 mL). Vials were sealed with Teflon caps and purged with nitrogen gas prior to storage at -20 °C. The kinetics of nitration was recorded for 2 h by taking aliquots (100 μL) 0.5, 15, 30, 45, 60, 90, and 120 min after addition of the nitrating reagent. Samples were analyzed immediately.

Nitration of cLa by P-NAP

An aliquot of cLa (75 μL; 8 mmol/L) was co-incubated with the photocontrollable peroxynitrite donor P-NAP (24 μL, 100 mmol/L in dimethylformamide) [33]. The open polypropylene tube containing the sample was placed under a UV lamp (Dr. Hönle, Gräfelfing, Germany) and irradiated (20 min) with monochromatic UV-A light (350 nm) with an average flux of 105 W/m^2. The kinetics of nitration was recorded for 2 h by taking aliquots (50 μL) 0, 3, 6, 9, 15, 30, 60, and 120 min after the reaction had started. Nitrated cLa was extracted using chloroform (100 μL), dried, and reconstituted in chloroform (50 μL). Samples were analyzed immediately.

Electrospray ionization LTQ Orbitrap MS of nitrated PUFA

Samples were diluted in a mixture of methanol and chloroform (2:1, v/v) containing ammonium formate (5 mmol/L) to obtain 10 μmol/L solutions [used for negative ion mode electrospray ionization (ESI) MS] or in a 5 mmol/L solution of lithium trifluoroacetate in methanol (positive ion mode ESI-MS). The samples were analyzed using a robotic nanoflow ion source (TriVersaNanoMate; AdvionBioSciences, Ithaca, NY, ZSA) equipped with a nanoelectrospray chip (-1.2-kV ionization voltage, 0.3-psi nitrogen backpressure for negative ion mode; 1.4-kV ionization voltage, 0.4-psi nitrogen backpressure for positive ion mode) coupled to an LTQ Orbitrap XL ETD mass spectrometer (Thermo Fischer Scientific, Bremen, Germany). The temperature of the transfer capillary was set to 200 °C and the tube lens voltage was set to 120 V. Mass spectra were acquired with the Orbitrap with a target mass resolution of 100,000 at *m*/*z* 400. Collision-induced dissociation (CID) and higher-energy CID (HCD) relied on an isolation width of 1.5 *u* and a normalized collision energy of 30 % (CID) and 42 % (HCD). Recorded data were analyzed manually using Xcalibur (version 2.0.7, Thermo Fisher).

PUFA nitration kinetics using MRM

Analyses were performed with as ESI 4000 QTRAP system (AB Sciex Germany, Darmstadt, Germany) operated in a negative ion mode with an ionization voltage of -4.5 kV, an entrance potential of -10 V, and an ion source temperature of 600 °C. The normalized collision energy, declustering potential, and exit quadrupole potential were optimized for each Q1/Q3 transition. The MRM included the two most intense transitions of each analyte with a dwell time of 40 ms. Each sample (30 μL in ESI solution) was infused with methanol (0.2 mL/min) using an Waters Alliance 2790 high-performance LC instrument (Waters, Eschborn, Germany) and measured in triplicate. Data were processed using Analyst (version 1.6, AB Sciex).

Analytical characterization of nitrated and oxidized PUFA in cardiomyocytes

In vitro nitration mixtures of Oa, La, Aa, Dha, and cLa were used to determine the retention times of all products. The LC–MRM was performed with a nanoACQUITY UPLC system (Waters, Eschborn, Germany) operated in high flow mode using the mixer kit for 1 mm columns (Waters, Eschborn, Germany) coupled to an ESI triple-quadrupole linear ion trap MS instrument (4000 QTRAP, AB Sciex Germany, Darmstadt, Germany). Samples were separated on an ACQUITY UPLC HSS T3 C_{18} column (internal diameter 1 mm, length 100 mm, pore size 100 Å, and particle size 1.8 μm) using a column temperature of 50 °C , a flow rate of 100 μL/min, and a linear 6-minute gradient from 30 % acetonitrile to 98 % acetonitrile in 0.1 % aqueous HCOOH. The electrospray voltage was set to -4.5 kV, the ion source temperature was set to 600 ° C, the entrance potential was set to -10 V, and the dwell time was set to 40 ms. All previously optimized transition pairs (declustering potential, collision energy, and exit quadrupole potential) of each analyte were included to record their retention times (see Table S1), whereas only the most sensitive and retention-time-specific transitions of each analyte were included in the final MRM method used for the relative quantification of nitrated and oxidized PUFA in the cardiomyocyte nitrosative stress model.

Cardiomyocyte cell culture and nitrosative stress induction

Primary rat cardiomyocytes (Innoprot, Elexalde Derio, Spain) were cultured until 80 % confluence in Dulbecco's modified Eagle's medium/Ham's F12 medium supplemented with fetal bovine serum (20 %), horse serum (5 %), L-glutamine (2 mmol/L), nonessential amino acids (0.1 mmol/L), sodium pyruvate (3 mmol/L), and antibiotics (1 %) at 37 °C (95 % air and 5 % CO_2 atmosphere). The medium was replaced with serum-free medium 24 h before treatment with 3-morpholinosydnonimine (SIN-1; 10 μmol/L, 15, 30, and 70 min). Untreated (control) and treated cells (around 1.5 × 10^6) were collected and washed with phosphate-buffered saline (pH 7.4), and lipids were extracted using MTBE [36]. Briefly, cell pellets were resuspended in 50 μL of ice-cold 0.1 % aqueous ammonium acetate containing 1 ng of internal standards (C_{21}-15-F_{2t}-IsoP, d_4-10-F_{4t}-NeuroP, d_4-4-RS-4-F_{4t}-NeuroP; Table S1). After 15 min on ice, 375 μL of methanol and 1.25 mL of MTBE were added, and the mixture was kept on a rotary shaker for 1 h at 4 °C. Separation of phases was achieved by adding water (313 μL) and keeping the mixture

on the rotary shaker for 10 min at 4 °C. After centrifugation (5 min, 4 °C, 1,000*g*) the upper, organic phase was collected and dried under a vacuum. The lower, aqueous phase was used to measure the protein concentration by a Bradford assay. Data were acquired and analyzed using Analyst (version 1.6).

Results and discussion

Mass-spectrometric analysis of fatty acids nitrated with NO_2BF_4

Nitronium tetrafluoroborate (NO_2BF_4) readily produces NO_2^+, which can nitrate PUFA by electrophilic substitution. Although nitration of fatty acids by NO_2BF_4 results in an array of different nitration products and not just a few positional nitration isomers, we used this approach because of its simplicity and the relatively high yields of nitrated PUFA. After 1 h nitration of Oa, La, Aa, and Dha, the sample mixtures were directly analyzed by ESI LTQ Orbitrap MS. The high resolution (HR) and mass accuracy provided elemental compositions of the detected nitration products (Table 1), including singly or multiply nitrated derivatives and nitro-oxidized species (Fig. 1). Fluorinated NO_2-FA, which were also observed as by-products, were not considered in the following study.

Nitration of Oa yielded ten signals corresponding to different reaction products of Oa (Fig. 1a). The signal of deprotonated Oa (*m*/*z* 281.25) was not observed, indicating that within 1 h of nitration, Oa was quantitatively consumed. Two low-intensity signals at *m*/*z* 295.23 and *m*/*z* 297.24 were assigned as keto-Oa (OaO) and hydroxy-Oa (OaOH), whereas the remaining eight signals, including the base peak, corresponded to nitrated or nitroslyated Oa. Detection of $OaNO_2$ (*m*/*z* 326.23), dinitro-Oa [$Oa(NO_2)_2$; *m*/*z* 371.22], and trinitro-Oa [$Oa(NO_2)_3$; *m*/*z* 416.20] showed that up to three NO_2 groups can be present although Oa contains only one double bond. Although electrophilic nitration is known to produce vinylnitro isomers, detection of $Oa(NO_2)_3$ after Oa nitration suggests the presence of allylic NO_2 groups. Signals with a mass shift of +29.99 u were assigned to nitroso-Oa (OaNO; *m*/*z* 310.24) and nitrosodinitro-Oa [$Oa(NO_2)_2NO$, *m*/*z* 398.19]. The signal at *m*/*z* 342.23 may indicate hydroxynitro-Oa ($OaNO_2OH$), an oxidized nitro species. Peaks corresponding to nitrooctadecadienoic acid [$La(NO_2)_2$, *m*/*z* 369.20] and nitrosonitrooctadecadienoic acid ($LaNO_2NO$; *m*/*z* 353.21) showed that Oa nitration can yield products containing two double bonds, such as octadecadienoic acid.

La nitration resulted in nine reaction products (Fig. 1b), including oxidized forms, such as keto-La (LaO; *m*/*z* 293.21) and hydroxy-La (LaOH; *m*/*z* 295.23). Notably, signals of the oxidized La were more intense then the signals of oxidized Oa species. The peak corresponding to deprotonated

Table 1 Summary of NO_2BF_4- and 2,3,5,6-tetramethyl-4-(methylnitrosoamino)phenol-mediated nitration products of oleic acid (*Oa*), linoleic acid (*La*), arachidonic acid (*Aa*), docosahexaenoic acid (*Dha*), and conjugated La (*cLa*). The elemental composition and the *m*/*z* values for deprotonated ions are shown

Fatty acid	Oxidation derivatives	Nitration derivatives			Nitration and oxidation derivatives	
	–OOH, –OH, =O	$(NO)_x$	$(NO_2)_x$	$(NO)_x(NO_2)_y$	$(NO_2)_x(OH)_y$	
Oa (18:1)	$C_{18}H_{31}O_3^-$ (*m*/*z* 295.2275), $C_{18}H_{33}O_3^-$ (*m*/*z* 297.2431)	$C_{18}H_{32}O_3N^-$(*m*/*z* 310.2390)	$C_{18}H_{32}O_4N^-$ (*m*/*z* 326.2332), $C_{18}H_{29}O_6N_2^-$ (*m*/*z* 369.2035), $C_{18}H_{31}O_6N_2^-$ (*m*/*z* 371.2188), $C_{18}H_{30}O_8N_3^-$ (*m*/*z* 416.2038)	$C_{18}H_{29}O_5N_2^-$ (*m*/*z* 353.2082), $C_{18}H_{28}O_7N_2^-$ (*m*/*z* 398.1932)	$C_{18}H_{32}O_5N^-$ (*m*/*z* 342.2289)	
La (18:2)	$C_{18}H_{29}O_3^-$ (*m*/*z* 293.2121), $C_{18}H_{31}O_3^-$ (*m*/*z* 295.2278)	$C_{18}H_{30}O_3N^-$ (*m*/*z* 308.2230)	$C_{18}H_{30}O_4N^-$ (*m*/*z* 324.2178), $C_{18}H_{29}O_6N_2^-$ (*m*/*z* 369.2029), $C_{18}H_{28}O_8N_3^-$ (*m*/*z* 414.1878), $C_{18}H_{27}O_{10}N_4^-$ (*m*/*z* 459.1727)	–	$C_{18}H_{30}O_5N^-$ (*m*/*z* 340.2131), $C_{18}H_{32}O_5N^-$ (*m*/*z* 342.2089)	
Aa (20:4)	$C_{20}H_{29}O_3^-$ (*m*/*z* 317.2278), $C_{20}H_{31}O_3^-$ (*m*/*z* 319.2275)	$C_{20}H_{30}O_3N^-$ (*m*/*z* 332.2230), $C_{20}H_{29}O_4N_2^-$ (*m*/*z* 361.2244)	$C_{20}H_{30}O_4N^-$ (*m*/*z* 348.2180), $C_{20}H_{29}O_6N_2^-$ (*m*/*z* 393.2032), $C_{20}H_{28}O_8N_3^-$ (*m*/*z* 438.1881)	$C_{20}H_{29}O_5N_2^-$ (*m*/*z* 377.2082)	$C_{20}H_{30}O_5N^-$ (*m*/*z* 364.2129)	
Dha (22:6)	$C_{22}H_{29}O_3^-$ (*m*/*z* 341.2114), $C_{22}H_{31}O_3^-$ (*m*/*z* 343.2271)	–	$C_{22}H_{30}O_4N^-$ (*m*/*z* 372.2178), $C_{22}H_{29}O_6N_2^-$ (*m*/*z* 417.2028), $C_{22}H_{28}O_8N_3^-$ (*m*/*z* 462.1878)	$C_{22}H_{29}O_5N_2^-$ (*m*/*z* 401.2079), $C_{22}H_{28}O_7N_3^-$ (*m*/*z* 446.1930)	$C_{22}H_{30}O_5N^-$ (*m*/*z* 388.2127), $C_{22}H_{31}O_7N_2^-$ (*m*/*z* 435.1773)	
cLa (18:2)	$C_{18}H_{29}O_3^-$ (*m*/*z* 293.2114), $C_{18}H_{31}O_3^-$ (*m*/*z* 295.2271), $C_{18}H_{31}O_4^-$ (*m*/*z* 311.2222), $C_{18}H_{33}O_4^-$ (*m*/*z* 313.2377)	$C_{18}H_{30}O_3N^-$ (*m*/*z* 308.2225)	$C_{18}H_{30}O_4N^-$ (*m*/*z* 324.2174), $C_{18}H_{29}O_6N_2^-$ (*m*/*z* 369.2025)	$C_{18}H_{31}O_5N_2^-$ (*m*/*z* 355.2233)	$C_{18}H_{30}O_5N^-$ (*m*/*z* 340.2123), $C_{18}H_{32}O_5N^-$ (*m*/*z* 342.2280), $C_{18}H_{32}O_6N^-$ (*m*/*z* 358.2229), $C_{18}H_{29}O_7N_2^-$ (*m*/*z* 385.1975)	

La was observed at *m/z* 279.23, indicating that La was not fully consumed within 1 h in the reaction with NO_2^+. Signals corresponding to $LaNO_2$ (*m/z* 324.22), dinitro-La [$La(NO_2)_2$; *m/z* 369.20], trinitro-La [$La(NO_2)_3$; *m/z* 414.19], and tetranitro-La [$La(NO_2)_4$; *m/z* 459.17] suggested that the two double bonds allowed incorporation of up to four nitro groups. Unlike Oa nitration, La nitration yielded only one nitroso product, observed at *m/z* 308.22 (LaNO). Similarly to Oa nitration, hydroxynitro-La ($LaNO_2OH$; *m/z* 340.21) and hydroxynitrooctadecenoic acid ($OaNO_2OH$; *m/z* 342.23) were also detected.

ESI Orbitrap mass spectra of Aa (Fig. 1c) and Dha (Fig. 1d) nitration mixtures displayed the deprotonated fatty acid ions as base peaks (*m/z* 303.23 and *m/z* 327.23, respectively), and the relative signal intensities of all nitration products were below 10 %. This observation indicated significantly lower susceptibilities of Aa and Dha to NO_2^+-mediated nitration compared with Oa and La. Both Aa and Dha were oxidized to keto derivatives (*m/z* 317.23, AaO; *m/z* 341.21, DhaO) and hydroxy derivatives (*m/z* 319.23, AaOH; *m/z* 343.23, DhaOH). Mass spectra of both Aa and Dha nitration mixtures revealed the presence of nitro derivatives (*m/z* 348.22, $AaNO_2$; *m/z* 372.22, $DhaNO_2$), dinitro derivatives [*m/z* 393.20, $Aa(NO_2)_2$; *m/z* 417.20, $Dha(NO_2)_2$], and trinitro derivatives [*m/z* 438.19, $Aa(NO_2)_3$; *m/z* 462.19, $Dha(NO_2)_3$]. Additionally, nitroso-Aa (AaNO; *m/z* 332.22), dinitro-Aa [$Aa(NO)_2$; *m/z* 361.22], and nitrosonitro-Aa ($AaNO_2NO$, *m/z* 377.21) as well as nitrosonitro-Dha ($DhaNO_2NO$, *m/z* 401.21) and nitrosodinitro-Dha [$Dha(NO_2)_2NO$, *m/z* 446.19] were detected. Weak signals were observed for nitro-oxidized Aa and Dha—namely, hydroxynitro-Aa ($AaNO_2OH$; *m/z* 364.21), hydroxynitro-Dha ($DhaNO_2OH$; *m/z* 388.21), and hydroxydinitrodocosapentaenoic acid [$Dpa(NO_2)_2OH$; *m/z* 435.18,].

Electrophilic fatty acid nitration by nitronium ions under low oxygen tension resulted in a high diversity of modified Oa, La, Aa, and Dha. ESI Orbitrap MS spectra acquired after a reaction time of 1 h (Fig. 1) revealed different susceptibilities. To the best of our knowledge, this is the first report on in vitro nitration of Dha. Besides single-nitro fatty acids, the formation of polynitro fatty acids was observed for each fatty acid. Regardless of a higher unsaturation degree of Aa (C20:4) and Dha (C22:6), these two fatty acids were detected with up to three nitro groups introduced along the alkyl chain, whereas for La with two double bonds even a tetranitro derivative was present. Our data indicate lower susceptibilities of Aa and Dha toward nitration in general and especially the formation of multiple nitration derivatives compared with Oa and La. The relative signal intensities of the modified species decreased with increasing fatty acid chain lengths and the numbers of double bonds in PUFA. Additionally, the low oxygen tension conditions applied here minimized formation of oxidized fatty acids and nitrohydroxy fatty acids.

MS/MS of NO_2-FA

The CID and HCD fragmentation behavior of nitrated PUFA was studied using HR-MS/MS in order to evaluate the diversity of positional isomers on the basis of previously published mechanisms [37] (see Figs. S1–S4, Scheme S1). Neutral loss of nitrous acid (HNO_2; -47 u) produced under the CID conditions was observed in all tandem mass spectra of NO_2-FA, and served as a reporter ion for the presence of the nitro group. Although successful nitration of Oa, La, and Aa and analysis of the corresponding MS/MS spectra was previously reported, to the best of our knowledge, this is the first report of Dha nitration. Since in the MS/MS spectrum of deprotonated $DhaNO_2$ the parent ion dominates the spectrum, and fragmentation of the alkyl chain was poor, we used the lithiated ion of $DhaNO_2$ for the fragmentation. We relied on the fragmentation mechanism previously reported by Bonacci et al. [37] to predict a series of fragment ions of each nitro-Dha ($DhaNO_2$) isomer, and compared them with the recorded Fourier transform CID-MS/MS spectrum (Fig. 2). It was possible to match 12 product ions, including structure-specific ions for seven nitro-Dha isomers, including 11-NO_2-Dha (*m/z* 161.08), 13-NO_2-Dha (*m/z* 175.09), 14-NO_2-Dha (*m/z* 201.11), 16-NO_2-Dha (*m/z* 215.12), 17-NO_2-Dha (*m/z* 241.14), 19-NO_2-Dha (*m/z* 255.16), and 20-NO_2-Dha (*m/z* 281.17). Fragment ions containing a nitrogen atom were not detected.

Similarly, the tandem mass spectrum of $[AaNO_2+Li^+]^+$ recorded using HCD fragmentation and detection in the Orbitrap mass analyzer (Fig. S2) confirmed the presence of five $AaNO_2$ vinyl isomers—namely, 9-NO_2-Aa, 11-NO_2-Aa, 12-NO_2-Aa, 14-NO_2-Aa, and 15-NO_2-Aa (Fig. S2, Scheme S1). We did not observe fragment ions specific for 5-NO_2-Aa, 6-NO_2-Aa, and 8-NO_2-Aa or 4-NO_2-Dha, 5-NO_2-Dha, 7-NO_2-Dha, 8- NO_2-Dha, and 10-NO_2-Dha. However, it cannot be ruled out that isomers of nitro fatty acids with the NO_2 group localized at the first three vinyl carbons are formed, but with lower yields compared with the other isomers, and thus the corresponding ions will result in signal intensities below the limit of detection of the Orbitrap mass analyzer. Furthermore, the fragmentation pattern might be different for the isomers with the NO_2 group near the carboxy group. Nevertheless, Trostchansky et al. [31] performed in vitro nitration of Aa by sodium nitrite under acidic conditions, and also observed only four major isomers of $nAaNO_2$—namely, 9-NO_2-Aa, 12-NO_2-Aa, 14-NO_2-Aa, and 15-NO_2-Aa.

Further, in vitro nitrated PUFA mixtures were used to optimize MRM parameters, including precursor to product ion transitions in a series of direct infusion experiments (Table S1). This in vitro approach allowed us to specify 91 different transition pairs for the simultaneous relative quantification of 42 nitrated, oxidized, and nitro-oxidized PUFA, which was further validated as part of the nitration kinetics study.

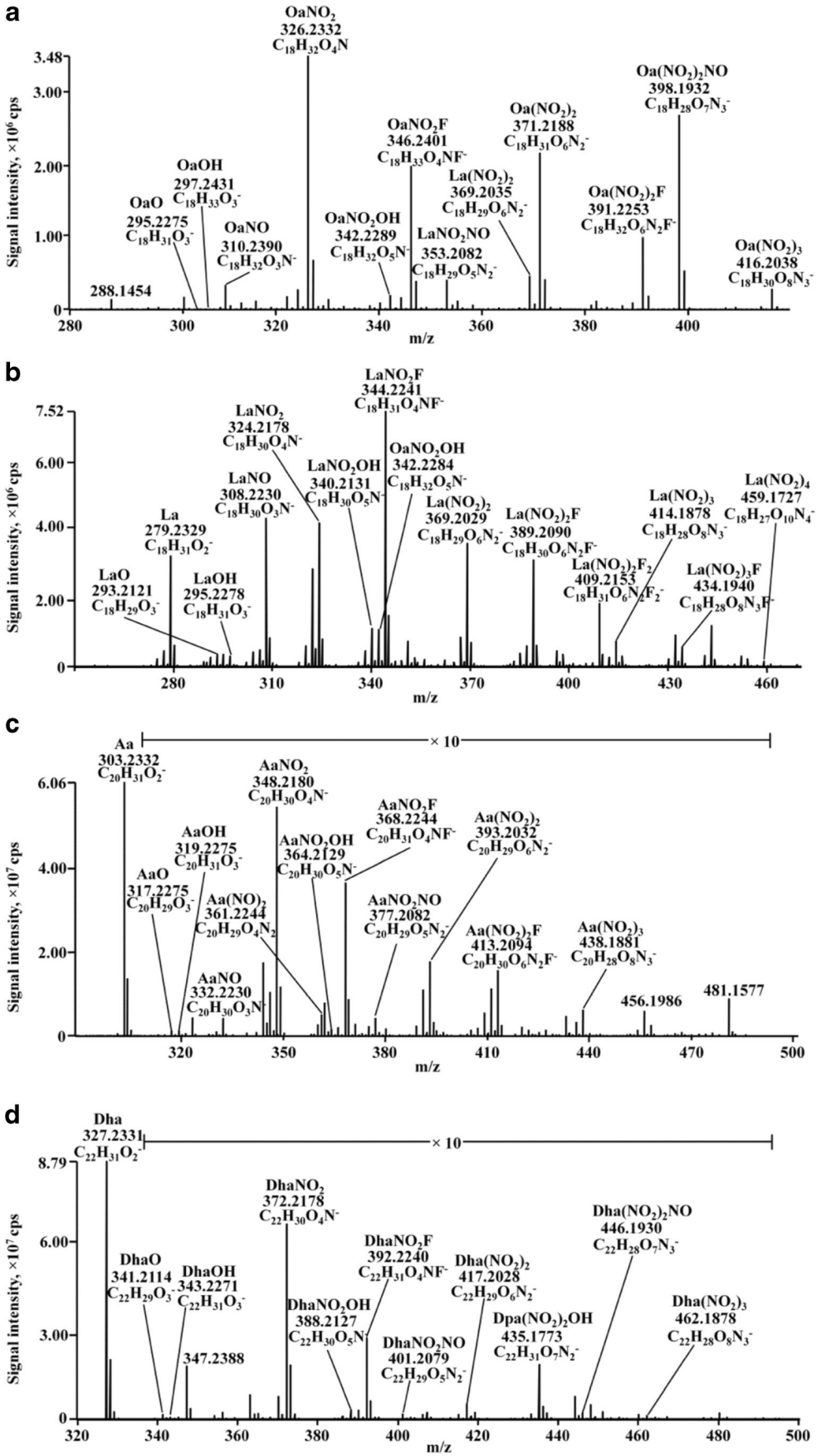
a
OaNO2
326.2332
C18H32O4N
Oa(NO2)2NO
398.1932
C18H28O7N3-
OaNO2F
346.2401
C18H33O4NF-
Oa(NO2)2
371.2188
C18H31O6N2-
OaOH
297.2431
C18H33O3-
La(NO2)2
369.2035
C18H29O6N2-
OaO
295.2275
C18H31O3-
Oa(NO2)2F
391.2253
C18H32O6N2F-
OaNO
310.2390
C18H32O3N-
OaNO2OH
342.2289
C18H32O5N-
LaNO2NO
353.2082
C18H29O5N2-
Oa(NO2)3
416.2038
C18H30O8N3-
288.1454
Signal intensity, ×10^6 cps
m/z
b
LaNO2F
344.2241
C18H31O4NF-
LaNO2
324.2178
C18H30O4N-
OaNO2OH
342.2284
C18H32O5N-
LaNO2OH
340.2131
C18H30O5N-
LaNO
308.2230
C18H30O3N-
La(NO2)4
459.1727
C18H27O10N4-
La(NO2)3
414.1878
C18H28O8N3-
La
279.2329
C18H31O2-
La(NO2)2
369.2029
C18H29O6N2-
La(NO2)2F
389.2090
C18H30O6N2F-
La(NO2)2F2
409.2153
C18H31O6N2F2-
La(NO2)3F
434.1940
C18H28O8N3F-
LaO
293.2121
C18H29O3-
LaOH
295.2278
C18H31O3-
Signal intensity, ×10^6 cps
m/z
c
Aa
303.2332
C20H31O2-
× 10
AaNO2
348.2180
C20H30O4N-
AaNO2F
368.2244
C20H31O4NF-
Aa(NO2)2
393.2032
C20H29O6N2-
AaOH
319.2275
C20H31O3-
AaNO2OH
364.2129
C20H30O5N-
AaO
317.2275
C20H29O3-
Aa(NO)2
361.2244
C20H29O4N2-
AaNO2NO
377.2082
C20H29O5N2-
Aa(NO2)2F
413.2094
C20H30O6N2F-
Aa(NO2)3
438.1881
C20H28O8N3-
AaNO
332.2230
C20H30O3N-
456.1986
481.1577
Signal intensity, ×10^7 cps
m/z
d
Dha
327.2331
C22H31O2-
× 10
DhaNO2
372.2178
C22H30O4N-
Dha(NO2)2NO
446.1930
C22H28O7N3-
DhaNO2F
392.2240
C22H31O4NF-
Dha(NO2)2
417.2028
C22H29O6N2-
DhaO
341.2114
C22H29O3-
DhaOH
343.2271
C22H31O3-
DhaNO2OH
388.2127
C22H30O5N-
Dpa(NO2)2OH
435.1773
C22H31O7N2-
Dha(NO2)3
462.1878
C22H28O8N3-
DhaNO2NO
401.2079
C22H29O5N2-
347.2388
Signal intensity, ×10^7 cps
m/z

◀ **Fig. 1** Electrospray ionization (ESI) Orbitrap mass spectrometry spectra recorded after 1 h of oleic acid (Oa; **a**), linoleic acid (La; **b**), arachidonic acid (Aa; **c**) and docosahexaenoic acid (Dha; **d**) nitration with nitronium tetrafluoroborate

Kinetics of NO_2^+-mediated nitration of Oa, La, Aa, and Dha

The kinetics of PUFA nitration by NO_2^+ was monitored by MRM-based ESI-MS/MS. Altogether, we were able to monitor eight, nine, eight, and five products of Oa, La, Aa, and Dha nitration and oxidation, respectively (see Figs S5–S8). Except for OaO, all monitored oxidized fatty acids (i.e., LaO, LaOH, AaO, AaOH, and DhaO) were formed immediately, and then their quantities decreased constantly, most likely due to further nitration by NO_2^+ ions. Among the singly nitrated derivatives, $OaNO_2$ was formed the fastest, with a mild increase over the following 60 min. The quantities of $LaNO_2$ and $AaNO_2$ increased several fold until the maxima were reached after 30 and 15 min, respectively, whereas the quantity of $DhaNO_2$ increased over the whole reaction period.

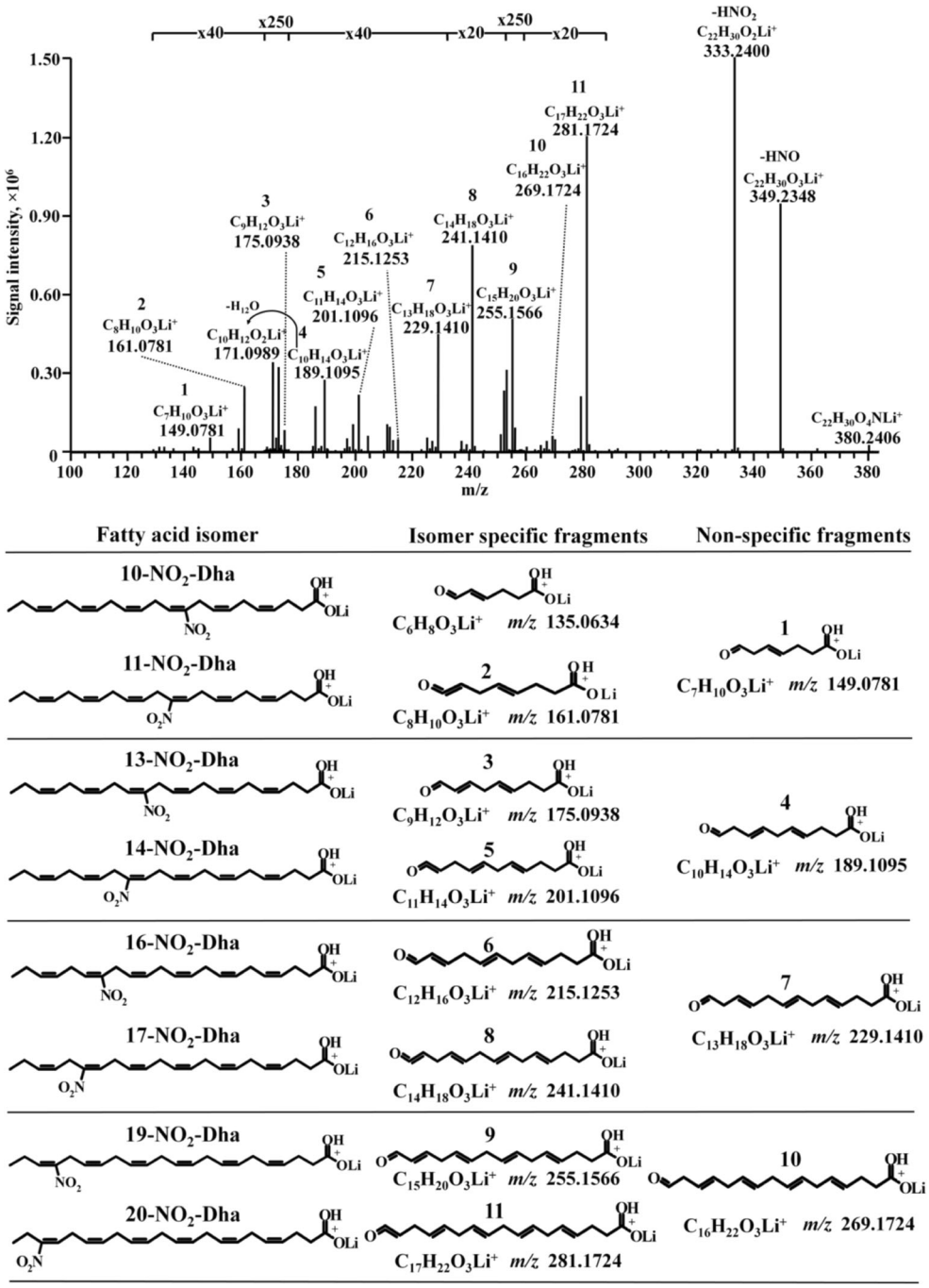

Fig. 2 ESI Fourier transform collision-induced dissociation spectrum of nitro-Dha (lithiated precursor at *m/z* 380.24; *upper panel*) and schematic annotation for structure-specific product ions (*1–11*; *lower panel*)

Nitro fatty acids via further reactions with NO_2^+ ions yield multiply nitrated fatty acids, which was observed for Oa, La, Aa, and Dha. The nitration kinetics revealed that Aa and Dha with longer alkyl chains and more double bonds than Oa and La are less reactive toward nitronium ions. Maximal levels of $Oa(NO_2)_2$ and $Aa(NO_2)_2$ were reached after 60 min, and the level of $La(NO_2)_2$ gradually increased over the reaction time course. The kinetics of $Dha(NO_2)_2$ formation suggests that the product is formed at the reaction onset and quantity decreases in the first 60 min. Finally, nitro-oxidized products of Oa and La ($OaNO_2OH$ and $LaNO_2OH$) showed an overall increase in the detected levels, whereas maximal levels of nitro-oxidized Aa and Dha ($AaNO_2OH$, $DhaNO_2OH$) were observed at the reaction onset, suggesting that the formed AaOH and DhaOH are readily consumed in further reactions with NO_2^+ ions.

HR-MS detection of cLa nitration by P-NAP

Use of the UV-inducible peroxynitrite donor P-NAP was recently introduced. It releases NO, which reacts under aerobic conditions with $O_2^{\bullet-}$, producing a peroxynitrite anion ($ONOO^-$) [33], which forms $\bullet NO_2$, an RNS capable of nitrating fatty acids in vivo or lipid radicals yielding nitro fatty acids and hydroxynitro fatty acids. Thus, we used P-NAP as an $ONOO^-$ donor in aqueous solutions to investigate fatty acid nitration for biologically more relevant conditions.

As a recent study identified cLa as a better substrate for nitration than bisallylic La in vitro and in vivo [12], we selected cLa as the substrate for P-NAP nitration (Fig. 3a). UV irradiation will induce peroxynitrite generation from P-NAP and additionally produce ROS, thus providing both ROS and RNS simultaneously, mimicking closely pathophysiological conditions. Signals corresponding to nitro-cLa ($cLaNO_2$; *m/z* 324.22) and dinitro-cLa [$cLa(NO_2)_2$; *m/z* 369.20] confirmed that P-NAP triggers free-radical-mediated nitration of cLa. Although $La(NO_2)_2$ is present with considerably lower relative signal intensities than after nitration of La by NO_2BF_4, the formation of $La(NO_2)_2$ by P-NAP suggests that multiple nitration derivatives can be formed via reaction with $\bullet NO_2$. Free-radical-mediated nitration of cLa under high oxygen tension yielded additionally four oxidation products—namely, keto-cLa (cLaO; *m/z* 293.21), hydroxy-cLa (cLaOH; *m/z* 295.23), hydroperoxy-cLa (cLaOOH; *m/z* 311.22), and hydroperoxyoctadecenoic acid (OaOOH; *m/z* 313.23). Among all the oxidation products, these showed the highest relative intensities. Moreover, several derivatives of cLa resulted from simultaneous oxidation and nitration, including hydroxynitro-cLa ($cLaNO_2OH$; *m/z* 340.21), hydroxynitrooctadecenoic acid ($OaNO_2OH$; *m/z* 342.23), hydroperoxynitrooctadecaenoic acid ($OaNO_2OOH$; *m/z* 358.22), and hydroxydinitro-cLa [$cLa(NO_2)_2OH$; *m/z* 385.20]. Additionally, nitroso derivatives were present after free-radical-mediated cLa nitration—namely, nitroso-cLa ($cLaNO$; *m/z* 308.22) and nitronitrosooctadecenoic acid ($OaNO_2NO$; *m/z* 355.22)—indicating that nitroso derivatives are most likely formed from nitro fatty acids, independently of the fatty acid nitration mechanism. cLa nitration mixtures were used for further optimization of the MRM method (Table S1).

The kinetics of nitration of cLa by P-NAP was monitored using specific MRM transitions of four oxidation, four nitration, and four nitro-oxidation products (Fig. 3b). UV irradiation of P-NAP readily releases $ONOO^-$ with tenfold increased levels within 15 min [33]. Thus, cLa nitration was monitored for shorter time intervals within the first 15 min (0, 3, 6, 9, and 15 min) and then for 30, 60, and 120 min of the nitration reaction. Conditions of higher oxygen tension favored fatty acid oxidation compared with the hydrophobic conditions of NO_2BF_4 nitration, yielding more oxidized $cLaNO_2$ derivatives. The concentrations of cLaOOH, cLaOH, cLaO, and OaOOH increased over the whole reaction period. Two main mechanisms have been proposed for free-radical-induced nitration of fatty acids [38]. One suggests the abstraction of a bisallylic hydrogen followed by the reaction with $\bullet NO_2$, producing vinylnitro isomers. The second mechanism predicts a homolytic attack of $\bullet NO_2$ at the C=C-bond, yielding a β-nitroalkyl radical that can lose a hydrogen atom and form nitroalkenes. Owing to the absence of bisallylic hydrogens in $cLaNO_2$, this product is most likely formed by the second mechanism. The kinetics of $cLaNO_2$ formation showed that maximal amounts of $cLaNO_2$ were reached after 6 min and then the amounts decreased rapidly until 15 min, reaching stable levels after 60 min. Indeed, this fast decrease between 6 and 15 min can be explained by the homolytic attack of a second $\bullet NO_2$ responsible for the increased levels of $cLa(NO_2)_2$ (maximum at 15 min). Similarly, $cLaNO_2$ can also react with $\bullet OH$ to form $cLaNO_2OH$ and $cLa(NO_2)_2OH$. Additionally, nitroalkyl radicals formed by the homolytic attack of a second $\bullet NO_2$ can produce a nitronitrite derivative, hydrolysis of which can further result in hydroxynitroalkenes, such as $OaNO_2OH$ and $OaNO_2OOH$. The formation rates of $cLaNO_2OH$ and $OaNO_2OH$ are clearly different. Whereas the $OaNO_2OH$ levels increase fast within the first 6 min, reaching relatively stable values, the $cLaNO_2OH$ and $cLa(NO_2)_2OH$ levels increase gradually over the full reaction period. The possibility that oxidized cLa is nitrated was also considered. The half-lives of $\bullet OH$ and $\bullet OOH$ (10^{-9} s) [39] are significantly shorter than the half-life of $\bullet NO_2$ (10^{-5}–10^{-4} s) [40]. Additionally, the reaction rates of an olefinic double bond with $\bullet OH$ and $\bullet OOH$ (10^8 M^{-1} s^{-1}) [39] are much faster than with

Fig. 3 (**a**) ESI Orbitrap mass spectrum of conjugated La (cLa) incubated with the peroxynitrite donor 2,3,5,6-tetramethyl-4-(methylnitrosoamino)phenol for 15 min. (**b**) Kinetics of cLa nitration monitored by multipole reaction monitoring (MRM) optimized for 12 cLa derivatives for 2 h

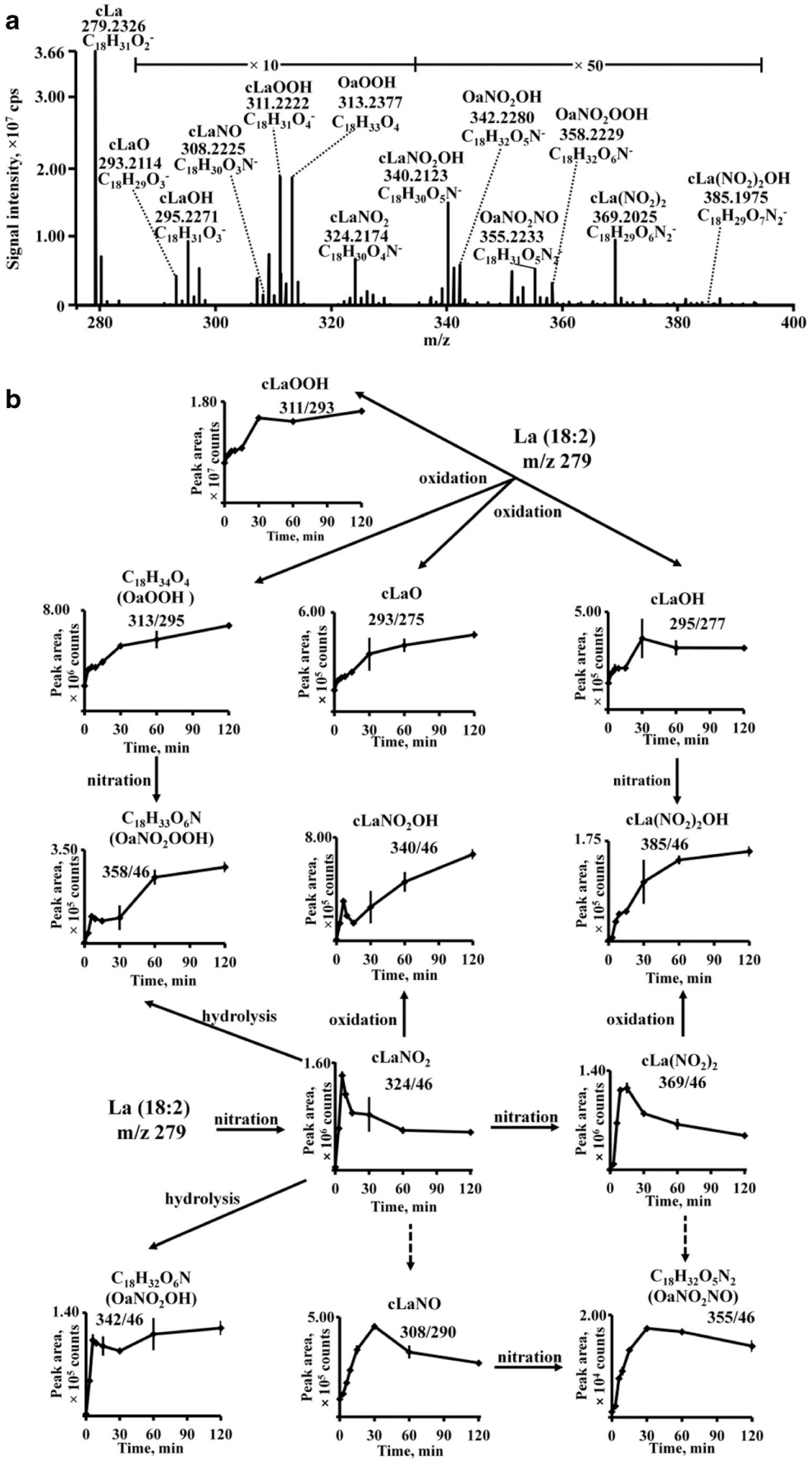
a
cLa
279.2326
C18H31O2-
× 10
× 50
cLaOOH
311.2222
C18H31O4-
OaOOH
313.2377
C18H33O4
OaNO2OH
342.2280
C18H32O5N-
OaNO2OOH
358.2229
C18H32O6N-
cLaNO
308.2225
C18H30O3N-
cLaO
293.2114
C18H29O3-
cLaNO2OH
340.2123
C18H30O5N-
cLaOH
295.2271
C18H31O3-
cLaNO2
324.2174
C18H30O4N-
OaNO2NO
355.2233
C18H31O5N2-
cLa(NO2)2
369.2025
C18H29O6N2-
cLa(NO2)2OH
385.1975
C18H29O7N2-
Signal intensity, ×10^7 cps
m/z
b
La (18:2)
m/z 279
oxidation
oxidation
cLaOOH
311/293
C18H34O4
(OaOOH)
313/295
cLaO
293/275
cLaOH
295/277
nitration
nitration
C18H33O6N
(OaNO2OOH)
358/46
cLaNO2OH
340/46
cLa(NO2)2OH
385/46
hydrolysis
oxidation
oxidation
La (18:2)
m/z 279
nitration
cLaNO2
324/46
cLa(NO2)2
369/46
nitration
hydrolysis
C18H32O6N
(OaNO2OH)
342/46
cLaNO
308/290
nitration
C18H32O5N2
(OaNO2NO)
355/46
Peak area, × 10^7 counts
Peak area, × 10^6 counts
Peak area, × 10^5 counts
Peak area, × 10^4 counts
Time, min

•NO_2 (10^6–10^7 M^{-1} s^{-1}) [40]. Thus, it appears very likely that oxidation occurs first and nitration follows. Both processes can produce $cLaNO_2OH$ and $cLa(NO_2)_2$, although their individual contributions remain to be defined. Hydroperoxy and hydroxy derivatives of NO_2-FA accumulate over time, and thus might provide a better "chemical fingerprint" of nitrosative stress than NO_2-FA itself. Finally, we observed formation of nitroso derivatives, including cLaNO and $OaNO_2NO$, reaching the highest concentrations after 30 min before decreasing afterward.

The kinetics of electrophilic (NO_2^+) and free radical (•NO_2) driven fatty acid nitrations are determined by the reaction conditions. Nevertheless, both electrophilic and free-radical-driven nitration of fatty acids successfully produced a wide array of products. Fatty acids nitrated with NO_2^+ under low oxygen tension yielded low levels of oxidized fatty acids, whereas high oxygen tension continuously produced oxidized fatty acids. Similar kinetics were observed for singly nitrated fatty acids for both nitration reactions, indicating that regardless of the nature of the RNS and the chemical environment, NO_2-FA do not represent the final products, but are prone to further nitration and oxidation reactions.

NO_2-FA in the cardiomyocyte nitrosative stress model

Following successful application of the new MRM method for simultaneous detection of nitrated and nitro-oxidized PUFA in kinetics experiments, we used this approach for relative quantification of modified PUFA in a cellular model of nitrosative stress using LC–MS coupling. Retention-time mapping was performed using each in vitro fatty acid nitration mixture separately and in combinations. Oxidation products with the same elemental composition (same *m/z* values) derived from different precursors, such as OaO and LaOH (*m/z* 295.2) have different functional groups (keto and hydroxy), and reversed-phase high-performance LC separation of these fatty acids results in different elution times of isobaric analytes, which allowed us to perform structure-specific retention-time mapping. Rat primary cardiomyocytes were treated with the peroxynitrite donor SIN-1 (10 μM) for 15, 30, and 70 min, and the levels of modified PUFA in lipid extracts were compared with those in untreated cells. The most sensitive MRM transitions optimized for each modified fatty acid were used (Table S1). Under the CID conditions, nitro fatty acids exhibit strong neutral loss of nitrous acid. Thus, for each nitration and oxidation/nitration derivative, the product ion of deprotonated nitrous acid (NO_2^-; *m/z* 46), and the product ions of single or multiple neutral losses of HNO_2 were monitored. These transitions were, without exception, more sensitive than any isomer-specific ones. Moreover, a fast reversed-phase LC gradient was designed, providing higher sensitivities owing to co-elution of different isomers. The specificity of the LC–MS method was ensured by compound-specific retention-time mapping using mixtures of in vitro nitrated fatty acids. Thus, identification of the free and modified fatty acids in the cell model was based on the retention time and quadrupole 1/quadrupole 3 specific transitions for each compound.

The stability of endogenous NO_2-FA is largely unknown. Owing to the absence of authentic isotopically labeled nitro fatty acid standards, we were unable to estimate compound stability or determine the limits of detection. Although artificial oxidation cannot be excluded, it is generally believed that the MTBE–methanol hydrophobic environment used here for lipid extraction in combination with low temperatures (4 °C) minimizes artificial oxidation of lipids. Nitro fatty acids were shown to be stabile under hydrophobic conditions, and organic extractions offer the highest recoveries of nitro fatty acids from samples [38]. Work by Baker et al. [15] indicates the level of $OaNO_2$ decays by 10 % when it is stored in methanol for 1 month, while 40 % loss was observed in phosphate buffer after 2 h. $LaNO_2$ showed higher instability, probably owing to the higher unsaturation degree. This indicates that $AaNO_2$ and $DhaNO_2$ might decay even faster than $OaNO_2$ and $LaNO_2$.

Apart from Oa, La, Aa and Dha, we detected and relatively quantified four oxidized fatty acids (OaOH, LaOH, LaOOH, AaOH), four NO_2-FA [$Oa(NO_2)_2$, $AaNO_2$, $DhaNO_2$, $Dha(NO_2)_2$] and two oxidized/nitrated fatty acids [$DhaNO_2OH$, $Dpa(NO_2)_2OH$] (Table 2, Figs. 4, S9). Induction of stress in the cardiomyocytes resulted in an increase in free fatty acid concentrations. After 15 min from stress onset, the levels of free La and Dha mildly increased (161 % and 155 % relative to the control for La and Dha, respectively; see Fig. S9), whereas approximately doubled levels of Oa and Aa (193 % for Oa; 183 % for Aa) were detected. An increase in the concentration of free fatty acids can be connected to elevated activity of phospholipase A_2 (PLA_2). Several studies showed that as a response to cell membrane lipid peroxidation, catalytic activity of PLA_2 is enhanced, leading to increases in the levels of free fatty acids and lysophospholipids [41, 42]. An increase in the levels of oxidized fatty acids in the first 30 min from stress onset was observed for La (168 % and 150 % for LaOH and LaOOH, respectively) and Aa (169 % for AaOH), whereas the highest increase was detected for OaOH (234 %). The increases in the levels of OaOH, LaOH, LaOOH, and AaOH in the first 30 min can be accounted for by direct PUFA oxidation as well as increased activities of PLA_2 that could lead to the hydrolysis of hydroxylated and peroxidized fatty acids from phospholipids.

The relatively fast LC gradient resulted in co-elution of the single-nitro fatty acid derivatives, whereas multiply nitrated fatty acids and nitro-oxidized fatty acids appeared as multiple signals in the in vitro nitration mixtures. In the SIN-1-treated

Table 2 Relative quantification of unmodified, oxidized, nitrated, and nitro-oxidized fatty acids detected after 15, 30, and 70 min of 3-morpholinosydnonimine treatment in rat primary cardiomyocytes shown as a percentage relative to the control (control=100 %)

Class	Analyte	15 min		30 min		70 min	
		Percentage relative to control±SD	*p*	Percentage relative to control±SD	*p*	Percentage relative to control±SD	*p*
Fatty acid	Oa	193±16	0.014	198±85	0.184	276±60	0.049
	La	161±22	0.012	184±18	0.0007	208±33	0.005
	Aa	183±30	0.012	171±22	0.006	171±27	0.015
	Dha	155±17	0.006	161±18	0.005	174±20	0.003
Oxidized fatty acid	OaOH	200±46	0.047	234±61	0.046	226±35	0.011
	LaOH	147±15	0.009	168±31	0.033	1,470±53	0.205
	LaOOH	117±3	0.011	150±14	0.036	164±64	0.221
	AaOH	163±12	0.0005	169±12	0.0002	157±21	0.014
Nitrated fatty acid	$Oa(NO_2)_2$	173±41	0.075	199±23	0.006	228±78	0.095
	$AaNO_2$	141±43	0.218	148±6	0.007	115±28	0.323
	$DhaNO_2$	174±45	0.121	230±32	0.028	190±55	0.122
	$Dha(NO_2)_2$	332±5	0.0002	371±40	0.011	226±22	0.014
Nitro-oxidized fatty acid	$DhaNO_2OH$	131±24	0.118	134±16	0.030	131±26	0.133
	$Dpa(NO_2)_2OH$	345±33	0.009	210±28	0.031	369±54	0.019

SD standard deviation

cardiomyocytes, the $Oa(NO_2)_2$-specific transition resulted in multiple signals at 5.82, 7.47, 7.98, 8.72, and 9.49 min (Fig. 4a). Using the retention-time mapping based on the in vitro NO_2^+ nitration of Oa, we were able to assign the peaks at 7.47 and 7.98 min to two $Oa(NO_2)_2$ isomers. After SIN-1 treatment, the levels of $Oa(NO_2)_2$ increased twofold compared with the levels in the untreated cells, reaching the maximal levels after 30 min from stress onset (199 %; Fig. 4a) and remained relatively stable after 70 min. $AaNO_2$ (retention time 8.33 min; Fig. 4b) and $DhaNO_2$ (retention time 8.53 min; Fig. 4c) reached maximal values after 30 min (148 % for $AaNO_2$; 230 % for $DhaNO_2$) of peroxynitrite treatment, followed by a mild decrease in the amounts detected.

Four signals (6.99, 7.65, 8.09, and 8.56 min) were detected for the $Dha(NO_2)_2$-specific transition for in vitro nitrated Dha (Fig. 4e). In the cardiomyocytes treated with SIN-1 for 15 min, two $Dha(NO_2)_2$ peaks with similar intensities were observed at 8.20 and 8.66 min, and were assigned to two different $Dha(NO_2)_2$ isomers. The levels of $Dha(NO_2)_2$ were significantly increased in the cardiomyocytes under the stress conditions compared with untreated cells, reaching the maximum at 30 min (371 %; Fig. 4e).

For in vitro nitrated Dha, multiple signals of $DhaNO_2OH$ (6.47, 7.23, and 8.09 min; Fig. 2d) and $Dpa(NO_2)_2OH$ (6.22, 6.86, 7.54, 8.17, and 9.50 min; Fig. 4f) were detected. However, in cardiomyocyte lipid extracts, only the single peak for each compound was present. Thus, $DhaNO_2OH$ was eluted at 7.30 min and $Dpa(NO_2)_2OH$ was eluted at 8.05 min. The concentration of $DhaNO_2OH$ in SIN-1-treated cells mildly increased within the first 15 min (131 %; Fig. 4d) and remained stable afterward. On the other hand, the levels of $Dpa(NO_2)_2OH$ significantly increased (345 %; Fig. 4f) at 15 min, decreased at 30 min (210 %), and again increased at 70 min (369 %).

Overall, treatment of primary cardiomyocytes with the peroxynitrite donor resulted in increased amounts of oxidized fatty acids (approximately 150 % compared with the untreated cells). The singly nitrated fatty acids—namely, $AaNO_2$ and $DhaNO_2$—were detected with maximal levels at 30 min, followed by a mild concentration decrease at 70 min. The relative increase in the level of $DhaNO_2$ (250 %) at 30 min of SIN-1 treatment was approximately three times higher than that of $AaNO_2$ (148 %). The levels of $Oa(NO_2)_2$ doubled after 30 min (199 %) and remained relatively stable afterward. Thus SIN-1 treatment of cardiomyocytes had the highest impact on the Dha nitration, resulting not only in pure nitration, but also in increased levels of nitration/oxidation derivatives. The highest and the fastest concentration increase of $Dpa(NO_2)_2OH$ (245 %) and $Dha(NO_2)_2$ (232 %) in SIN-1-treated cells compared with the untreated cells was detected after 15 min of stress induction. These results indicate that multiply nitrated and nitro-oxidized derivatives of fatty acids, including Dha, are produced in cells even under basal conditions, and the levels are significantly elevated in the peroxynitrite stress model. To the best of our knowledge, this is the first report of the endogenous formation of $AaNO_2$, and Dha nitration products such as $DhaNO_2$, $Dha(NO_2)_2$, $DhaNO_2OH$, and $Dpa(NO_2)_2OH$.

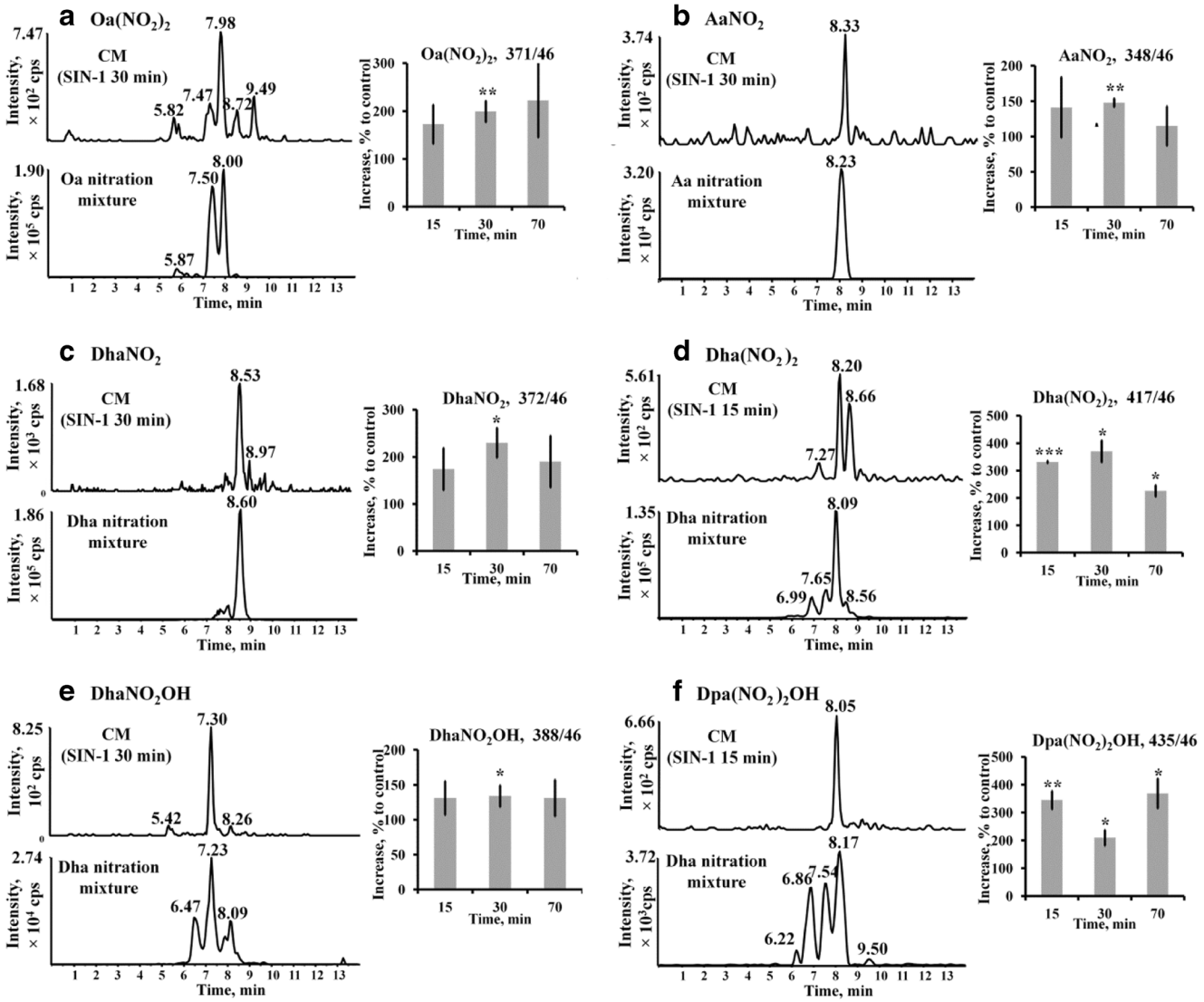

Fig. 4 Extracted ion chromatograms for the quadrupole 1/quadrupole 3 transition pairs corresponding to **a** $Oa(NO_2)_2$, **b** $AaNO_2$, **c** $DhaNO_2$, **d** $DhaNO_2OH$, **e** $Dha(NO_2)_2$, and **f** $Dpa(NO_2)_2OH$ in cardiomyocyte (CM) lipid extract (*upper panels*) and corresponding polyunsaturated fatty acids in in vitro nitration mixtures (*lower panels*). Identification of modified fatty acids was based on the compound-specific MRM transitions and retention times. Measured values were normalized to the values for the corresponding controls (100 %), averaged, and represented as bar plots with standard errors. The data represent the mean value of up to five independent measurements. Significant increase in quantified values [control vs 3-morpholinosydnonimine (*SIN-1*)-treated cells] was assigned using a *t* test (*one asterisk* $p<0.05$, *two asterisks* $p<0.01$, *three asterisks* $p<0.005$)

The presence of the endogenously formed NO_2-FA was reported for the first time more than a decade ago [9]. Several LC–MS/MS and gas chromatography–MS/MS studies have been directed toward quantification of $LaNO_2$ and $OaNO_2$ in human blood plasma, and reported values between 300 pmol/L [9–11, 13] and 600 nmol/L [14, 15], whereas $AaNO_2$ remained undetected [10]. Recently, Bonnaci et al. [12] showed that dietary cLa rather than bisallylic La is a preferential substrate for the nitration by $ONOO^-$ and $^{\bullet}NO_2$, with endogenous levels 0.3 to 1.3 nmol/L in healthy human plasma. In the present study, we did not observe detectable levels of $LaNO_2$, $cLaNO_2$, and $OaNO_2$ in control and SIN-1-treated rat cardiomyocytes, most probably owing to the low concentrations and/or absence of cLa as a nitration substrate in the cell culture medium. Additionally, nitroalkylation of proteins and glutathione by the electrophilic NO_2-FA and fatty acid metabolism can reduce endogenous levels of free NO_2-FA [43]. Over the past two decades various techniques have been designed for the enrichment of the low endogenous concentrations of Aa-derived F_2-isoprostanes (approximately 10^2 pmol/L in healthy human plasma) from various biological samples [44], and now ensure their routine detection and quantification by LC–MS. Biological concentrations of isoprostanes are similar to those of NO_2-FA in healthy human plasma; thus, further development of NO_2-FA enrichment protocols could improve their detection in biological samples.

In the present study, Dha-derived nitration products were detected for the first time. Although F_4-neuroprostanes derived from Dha, like Aa derived F_2-isoprostanes, have been related to various cardiovascular and neurodegenerative disorders [45, 46], here we can only speculate about the beneficial effects of Dha-derived nitration products, as was shown for $AaNO_2$ [27, 31, 32] and all other singly nitrated fatty acids. Lipid peroxidation products usually posses proinflammatory properties [47]; however current data on biological activities of NO_2-FA support their anti-inflammatory effects via both cGMP-dependent and cGMP-independent mechanisms. Although the overproduction of NO_2-FA was observed during inflammation, a series of anti-inflammatory effects were reported for $LaNO_2$ [48–50] , $OaNO_2$ [15, 24], and $AaNO_2$ [27, 31, 32]. The question about biological activities of multiply nitrated and nitro-oxidized PUFA remains open owing to the lack of the data on their biological availability.

Conclusion

A novel analytical approach to explore the diversity of NO_2-FA was developed using in vitro nitration mixtures of Oa, La, Aa, and Dha for optimization of highly specific and sensitive targeted LC–ESI-MS/MS. Specific MRM transitions were optimized for 42 reaction products—that is, singly and multiply nitrated as well as nitro-oxidized fatty acids. The optimized methods were applied for the detection and relative quantification of NO_2-FA in a cardiomyocyte model of nitrosative stress. Six fatty acid nitration products—namely, $Oa(NO_2)_2$, $AaNO_2$, $DhaNO_2$, $Dha(NO_2)_2$, $DhaNO_2OH$, and $Dpa(NO_2)_2OH$—were detected and quantified over a period of 70 min after stress induction, providing the kinetics of NO_2-FA formed in cells during nitrosative stress.

Acknowledgments The authors are grateful to Ralf Hoffmann (Institute of Bioanalytical Chemistry, University of Leipzig) for providing access to his laboratories and instruments. Financial support from the European Regional Development Fund (European Union and the Free State of Saxony; 100146238 and 100121468 to M.F.) and a stipend to I.M. provided by Universität Leipzig are gratefully acknowledged.

Authors' contributions I.M. performed all experimental work, corresponding data evaluation, and contributed to the writing of the manuscript. E.G. and V.V. designed the cell model of nitrosative stress and performed cell culture experiments. N.I., H.N., and N.M. provided the peroxynitrite donor 2,3,5,6-tetramethyl-4-(methylnitrosoamino)phenol. J.M.G., C.O., and T.D. provided internal standards used for liquid chromatography–tandem mass pectrometry. M.F. conceived and designed all experiments and contributed to the writing of the manuscript.

References

1. Pacher P, Beckman JS, Liaudet L (2007) Nitric oxide and peroxynitrite in health and disease. Physiol Rev 87(1):315–424
2. Wink DA, Hines HB, Cheng RYS, Switzer CH, Flores-Santana W, Vitek MP, Ridnour LA, Colton CA (2011) Nitric oxide and redox mechanisms in the immune response. J Leukoc Biol 89(6):873–891
3. Wang GR, Zhu Y, Halushka PV, Lincoln TM, Mendelsohn ME (1998) Mechanism of platelet inhibition by nitric oxide: in vivo phosphorylation of thromboxane receptor by cyclic GMP-dependent protein kinase. Proc Natl Acad Sci U S A 95(9):4888–4893
4. Riddell DR, Owen JS (1999) Nitric oxide and platelet aggregation. Vitam Horm 57:25–48
5. Kubes P, Suzuki M, Granger DN (1991) Nitric oxide: an endogenous modulator of leukocyte adhesion. Proc Natl Acad Sci U S A 88(11):4651–4655
6. Bloodsworth A, O'Donnell VB, Freeman BA (2000) Nitric oxide regulation of free radical- and enzyme-mediated lipid and lipoprotein oxidation. Arterioscler Thrombn Vasc Biol 20(7):1707–1715
7. Liu X, Miller MJ, Joshi MS, Thomas DD, Lancaster JR Jr (1998) Accelerated reaction of nitric oxide with O2 within the hydrophobic interior of biological membranes. Proc Natl Acad Sci U S A 95(5): 2175–2179
8. Moller MN, Li Q, Vitturi DA, Robinson JM, Lancaster JR Jr, Denicola A (2007) Membrane "lens" effect: focusing the formation of reactive nitrogen oxides from the $^{\bullet}NO/O_2$ reaction. Chem Res Toxicol 20(4):709–714
9. Lima ES, Di Mascio P, Rubbo H, Abdalla DS (2002) Characterization of linoleic acid nitration in human blood plasma by mass spectrometry. Biochemistry 41(34):10717–10722
10. Tsikas D, Zoerner AA, Mitschke A, Gutzki FM (2009) Nitro-fatty acids occur in human plasma in the picomolar range: a targeted nitro-lipidomics GC-MS/MS study. Lipids 44(9):855–865
11. Trettin A, Bohmer A, Zoerner AA, Gutzki FM, Jordan J, Tsikas D (2014) GC-MS/MS and LC-MS/MS studies on unlabelled and deuterium-labelled oleic acid (C18:1) reactions with peroxynitrite (O=N-O-O(-)) in buffer and hemolysate support the pM/nM-range of nitro-oleic acids in human plasma. J Chromatogr B Anal Technol Biomed Life Sci 964:172–179
12. Bonacci G, Baker PR, Salvatore SR, Shores D, Khoo NK, Koenitzer JR, Vitturi DA, Woodcock SR, Golin-Bisello F, Cole MP, Watkins S, St Croix C, Batthyany CI, Freeman BA, Schopfer FJ (2012) Conjugated linoleic acid is a preferential substrate for fatty acid nitration. J Biol Chem 287(53):44071–44082
13. Tsikas D, Zoerner A, Mitschke A, Homsi Y, Gutzki FM, Jordan J (2009) Specific GC-MS/MS stable-isotope dilution methodology for free 9- and 10-nitro-oleic acid in human plasma challenges previous LC-MS/MS reports. J Chromatogr B Anal Technol Biomed Life Sci 877(26):2895–2908
14. Baker PR, Schopfer FJ, Sweeney S, Freeman BA (2004) Red cell membrane and plasma linoleic acid nitration products: synthesis, clinical identification, and quantitation. Proc Natl Acad Sci U S A 101(32):11577–11582
15. Baker PR, Lin Y, Schopfer FJ, Woodcock SR, Groeger AL, Batthyany C, Sweeney S, Long MH, Iles KE, Baker LM, Branchaud BP, Chen YE, Freeman BA (2005) Fatty acid transduction of nitric oxide signaling: multiple nitrated unsaturated fatty acid derivatives exist in human blood and urine and serve as endogenous peroxisome proliferator-activated receptor ligands. J Biol Chem 280(51):42464–42475
16. Salvatore SR, Vitturi DA, Baker PR, Bonacci G, Koenitzer JR, Woodcock SR, Freeman BA, Schopfer FJ (2013) Characterization and quantification of endogenous fatty acid nitroalkene metabolites in human urine. J Lipid Res 54(7):1998–2009

17. Ferreira AM, Ferrari MI, Trostchansky A, Batthyany C, Souza JM, Alvarez MN, Lopez GV, Baker PR, Schopfer FJ, O'Donnell V, Freeman BA, Rubbo H (2009) Macrophage activation induces formation of the anti-inflammatory lipid cholesteryl-nitrolinoleate. Biochem J 417(1):223–234
18. Nadtochiy SM, Baker PR, Freeman BA, Brookes PS (2009) Mitochondrial nitroalkene formation and mild uncoupling in ischaemic preconditioning: implications for cardioprotection. Cardiovasc Res 82(2):333–340
19. Khoo NK, Freeman BA (2010) Electrophilic nitro-fatty acids: anti-inflammatory mediators in the vascular compartment. Curr Opin Pharmacol 10(2):179–184
20. Rubbo H (2013) Nitro-fatty acids: novel anti-inflammatory lipid mediators. Braz J Med Biol Res 46(9):728–734
21. Freeman BA, Baker PR, Schopfer FJ, Woodcock SR, Napolitano A, d'Ischia M (2008) Nitro-fatty acid formation and signaling. J Biol Chem 283(23):15515–15519
22. Ferreira AM, Minarrieta L, Lamas Bervejillo M, Rubbo H (2012) Nitro-fatty acids as novel electrophilic ligands for peroxisome proliferator-activated receptors. Free Radic Biol Med 53(9): 1654–1663
23. Li Y, Paonessa JD, Zhang Y (2012) Mechanism of chemical activation of Nrf2. PLoS ONE 7(4), e35122
24. Kansanen E, Bonacci G, Schopfer FJ, Kuosmanen SM, Tong KI, Leinonen H, Woodcock SR, Yamamoto M, Carlberg C, Yla-Herttuala S, Freeman BA, Levonen AL (2011) Electrophilic nitro-fatty acids activate NRF2 by a KEAP1 cysteine 151-independent mechanism. J Biol Chem 286(16):14019–14027
25. Wright MM, Schopfer FJ, Baker PR, Vidyasagar V, Powell P, Chumley P, Iles KE, Freeman BA, Agarwal A (2006) Fatty acid transduction of nitric oxide signaling: nitrolinoleic acid potently activates endothelial heme oxygenase 1 expression. Proc Natl Acad Sci U S A 103(11):4299–4304
26. Trostchansky A, Bonilla L, Thomas CP, O'Donnell VB, Marnett LJ, Radi R, Rubbo H (2011) Nitroarachidonic acid, a novel peroxidase inhibitor of prostaglandin endoperoxide H synthases 1 and 2. J Biol Chem 286(15):12891–12900
27. Gonzalez-Perilli L, Alvarez MN, Prolo C, Radi R, Rubbo H, Trostchansky A (2013) Nitroarachidonic acid prevents NADPH oxidase assembly and superoxide radical production in activated macrophages. Free Radic Biol Med 58:126–133
28. Klinke A, Moller A, Pekarova M, Ravekes T, Friedrichs K, Berlin M, Scheu KM, Kubala L, Kolarova H, Ambrozova G, Schermuly RT, Woodcock SR, Freeman BA, Rosenkranz S, Baldus S, Rudolph V, Rudolph TK (2014) Protective effects of 10-nitro-oleic acid in a hypoxia-induced murine model of pulmonary hypertension. Am J Respir Cell Mol Biol 51(1):155–162
29. Rudolph TK, Rudolph V, Edreira MM, Cole MP, Bonacci G, Schopfer FJ, Woodcock SR, Franek A, Pekarova M, Khoo NKH, Hasty AH, Baldus S, Freeman BA (2010) Nitro–fatty acids reduce atherosclerosis in apolipoprotein E–deficient mice. Arterioscler Thromb Vasc Biol 30(5):938–945
30. Zheng R, Heck DE, Black AT, Gow A, Laskin DL, Laskin JD (2014) Regulation of keratinocyte expression of stress proteins and antioxidants by the electrophilic nitrofatty acids 9- and 10-nitrooleic acid. Free Radic Bol Med 67:1–9
31. Trostchansky A, Souza JM, Ferreira A, Ferrari M, Blanco F, Trujillo M, Castro D, Cerecetto H, Baker PR, O'Donnell VB, Rubbo H (2007) Synthesis, isomer characterization, and anti-inflammatory properties of nitroarachidonate. Biochemistry 46(15):4645–4653
32. Bonilla L, O'Donnell VB, Clark SR, Rubbo H, Trostchansky A (2013) Regulation of protein kinase C by nitroarachidonic acid: impact on human platelet activation. Arch Biochem Biophys 533(1-2):55–61
33. Ieda N, Nakagawa H, Peng T, Yang D, Suzuki T, Miyata N (2012) Photocontrollable peroxynitrite generator based on N-methyl-N-nitrosoaminophenol for cellular application. J Am Chem Soc 134(5):2563–2568
34. Guy A, Oger C, Heppekausen J, Signorini C, De Felice C, Furstner A, Durand T, Galano JM (2014) Oxygenated metabolites of n-3 polyunsaturated fatty acids as potential oxidative stress biomarkers: total synthesis of 8-F_{3t}-IsoP, 10-F_{4t}-NeuroP and [D_4]-10-F_{4t}-NeuroP. Chemistry 20(21):6374–6380
35. Oger C, Bultel-Ponce V, Guy A, Balas L, Rossi JC, Durand T, Galano JM (2010) The handy use of Brown's P2-Ni catalyst for a skipped diyne deuteration: application to the synthesis of a [D_4]-labeled F_{4t}-neuroprostane. Chemistry 16(47):13976–13980
36. Matyash V, Liebisch G, Kurzchalia TV, Shevchenko A, Schwudke D (2008) Lipid extraction by methyl-tert-butyl ether for high-throughput lipidomics. J Lipid Res 49(5):1137–1146
37. Bonacci G, Asciutto EK, Woodcock SR, Salvatore SR, Freeman BA, Schopfer FJ (2011) Gas-phase fragmentation analysis of nitro-fatty acids. J Am Soc Mass Spectrom 22(9):1534–1551
38. Woodcock SR, Bonacci G, Gelhaus SL, Schopfer FJ (2013) Nitrated fatty acids: synthesis and measurement. Free Radic Biol Med 59:14–26
39. Halliwell B, Gutteridge JMC (1999) Free radicals in biology and medicine, 3rd edn. Clarendon Press, Oxford
40. Huie RE (1994) The reaction kinetics of NO_2. Toxicology 89(3): 193–216
41. Jezek J, Jaburek M, Zelenka J, Jezek P (2010) Mitochondrial phospholipase A2 activated by reactive oxygen species in heart mitochondria induces mild uncoupling. Physiol Res 59(5):737–747
42. Rashba-Step J, Tatoyan A, Duncan R, Ann D, Pushpa-Rehka TR, Sevanian A (1997) Phospholipid peroxidation induces cytosolic phospholipase A2 activity: membrane effects versus enzyme phosphorylation. Arch Biochem Biophys 343(1):44–54
43. Tsikas D, Zoerner AA, Jordan J (2011) Oxidized and nitrated oleic acid in biological systems: analysis by GC-MS/MS and LC-MS/MS, and biological significance. Biochim Biophys Acta 1811(11): 694–705
44. Milne GL, Musiek ES, Morrow JD (2005) F2-isoprostanes as markers of oxidative stress in vivo: an overview. Biomarkers 10(Suppl 1):S10–S23
45. Montuschi P, Barnes PJ, Roberts LJ (2004) Isoprostanes: markers and mediators of oxidative stress. FASEB J 18(15):1791–1800
46. Ricciotti E, FitzGerald GA (2011) Prostaglandins and Inflammation. Arterioscler Thromb Vasc Biol 31(5):986–1000
47. Lee SE, Park YS (2013) Role of lipid peroxidation-derived α, ß-unsaturated aldehydes in vascular dysfunction. Oxid Med Cell Longev 2013:629028
48. Lim DG, Sweeney S, Bloodsworth A, White CR, Chumley PH, Krishna NR, Schopfer F, O'Donnell VB, Eiserich JP, Freeman BA (2002) Nitrolinoleate, a nitric oxide-derived mediator of cell function: synthesis, characterization, and vasomotor activity. Proc Natl Acad Sci U S A 99(25):15941–15946
49. Coles B, Bloodsworth A, Eiserich JP, Coffey MJ, McLoughlin RM, Giddings JC, Lewis MJ, Haslam RJ, Freeman BA, O'Donnell VB (2002) Nitrolinoleate inhibits platelet activation by attenuating calcium mobilization and inducing phosphorylation of vasodilator-stimulated phosphoprotein through elevation of cAMP. J Biol Chem 277(8):5832–5840

50. Coles B, Bloodsworth A, Clark SR, Lewis MJ, Cross AR, Freeman BA, O'Donnell VB (2002) Nitrolinoleate inhibits superoxide generation, degranulation, and integrin expression by human neutrophils: novel antiinflammatory properties of nitric oxide-derived reactive species in vascular cells. Circ Res 91(5):375–381

Ivana Milic is a PhD candidate in the Institute of Bioanalytical Chemistry, Faculty of Chemistry and Mineralogy, at the University of Leipzig. Her research is focused on the development of liquid chromatography–mass spectrometry-based protocols for analysis of oxidized lipids and lipid–protein adducts.

Eva Griesser is a PhD candidate in the Institute of Bioanalytical Chemistry, Faculty of Chemistry and Mineralogy, at the University of Leipzig. Her research is focused on protein and lipid modifications in various cellular models of oxidative stress.

Venukumar Vemula is a PhD candidate in the Institute of Bioanalytical Chemistry, Faculty of Chemistry and Mineralogy, at the University of Leipzig. His research is focused on proteomic and lipidomic analysis of biomolecules oxidation.

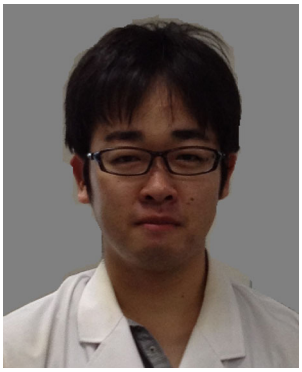

Naoya Ieda is an assistant professor of organic and medicinal chemistry in the Graduate School of Pharmaceutical Sciences, Nagoya City University. He has been working for several years on the development of photocontrollable reactive nitrogen species releasers as biological research tools or novel photodynamic therapy drug candidates.

Hidehiko Nakagawa is Head of the Laboratory of Organic and Medicinal Chemistry, Graduate School of Pharmaceutical Sciences, Nagoya City University. He has been working on the development of photocontrollable NO and related reactive nitrogen species, as well as the development of chemical tools for medicinal chemistry.

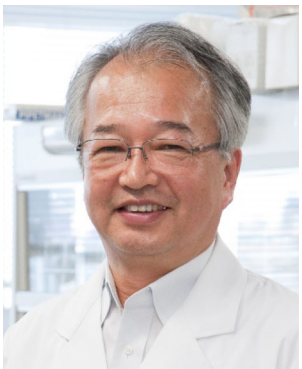

Naoki Miyata is a professor in the Institute of Drug Discovery Science of the Graduate School of Pharmaceutical Sciences, Nagoya City University. His research interests are chemical biology focused on reactive oxygen species and reactive nitrogen species, and also medicinal chemistry to develop useful enzyme inhibitors for the treatment of cancer and neurodegenerative disorders. His research is always based on organic chemistry.

Jean-Marie Galano studied chemistry at Paul Cézanne Université Marseille and obtained his PhD degree in the field of total synthesis under the supervision of Honoré Monti in 2001. He then moved to the University of Oxford to pursue a postdoctoral fellowship with David H. Hodgson on the development of new methods for the total synthesis of natural products. In October 2005 he joined the CNRS as a *chargé de recherche* at the University of Montpellier. His research focuses on new methods and strategies toward the total synthesis of natural products.

Thierry Durand is a group leader at the Institute of Biomolécules Max Mousseron. His research interests include the total synthesis of oxygenated cyclic and noncyclic metabolites of polyunsaturated fatty acids, mainly leukotrienes, isoprostanes, phytoprostanes, and neuroprostanes, as well as dihydroxylated polyunsaturated fatty acids, and the understanding of the role of such bioactive lipids by developing collaborations with chemists, biochemists, biologists, and clinicians all over the word.

Camille Oger obtained her PhD degree in organic synthesis in 2010 and is currently an assistant professor in organic chemistry in the University of Montpellier. Her research mainly focuses on the synthesis of lipid metabolites and their identification/quantitation in biological fluids as well as the discovery of biological properties.

Maria Fedorova is a group leader in the Institute of Bioanalytical Chemistry, Faculty of Chemistry and Mineralogy, at the University of Leipzig. Her research is focused on analysis of oxidized lipids and proteins as well as lipid–protein adducts in variety of in vitro and in vivo systems.